Identification and Characterization of (1*R*,6*R*)-2-Succinyl-6-hydroxy-2,4-cyclohexadiene-1-carboxylate Synthase in the Menaquinone Biosynthesis of *Escherichia coli*[†]

Ming Jiang, Xiaolei Chen, Zu-Feng Guo, Yang Cao, Minjiao Chen, and Zhihong Guo*

Department of Chemistry, Center for Cancer Research, The Hong Kong University of Science and Technology (HKUST), Clear Water Bay, Kowloon, Hong Kong Special Administrative Region (SAR), China

Received December 5, 2007; Revised Manuscript Received January 15, 2008

ABSTRACT: Menaquinone is a lipid-soluble molecule that plays an essential role as an electron carrier in the respiratory chain of many bacteria. We have previously shown that its biosynthesis in *Escherichia coli* involves a new intermediate, 2-succinyl-5-enolpyruvyl-6-hydroxy-3-cyclohexene-1-carboxylate (SEPHCHC), and requires an additional enzyme to convert this intermediate into (1*R*,6*R*)-2-succinyl-6-hydroxy-2,4-cyclohexadiene-1-carboxylate (SHCHC). Here, we report the identification and characterization of MenH (or YfbB), an enzyme previously proposed to catalyze a late step in menaquinone biosynthesis, as the SHCHC synthase. The synthase catalyzes a proton abstraction reaction that results in 2,5-elimination of pyruvate from SEPHCHC and the formation of SHCHC. It is an efficient enzyme ($k_{cat}/K_M = 2.0 \times 10^7$ M^{-1} s^{-1}) that provides a smaller transition-state stabilization than other enzymes catalyzing proton abstraction from carbon acids. Despite its lack of the proposed thioesterase activity, the SHCHC synthase is homologous to the well-characterized C−C bond hydrolase MhpC. The crystallographic structure of the *Vibrio cholerae* MenH protein closely resembles that of MhpC and contains a Ser-His-Asp triad typical of serine proteases. Interestingly, this triad is conserved in all MenH proteins and is essential for the SHCHC synthase activity. Mutational analysis found that the catalytic efficiency of the *E. coli* protein is reduced by 1.4×10^3, 2.1×10^5, and 9.3×10^3 folds when alanine replaces serine, histidine, and aspartate of the triad, respectively. These results show that the SHCHC synthase is closely related to α/β hydrolases but catalyzes a reaction mechanistically distinct from all known hydrolase reactions.

Menaquinone, or vitamin K_2, is a respiratory chain electron carrier essential to many microorganisms (*1, 2*). Its biosynthesis from chorismate of the shikimate pathway is an attractive target for development of new antibiotics against microbial pathogens (*3–5*). However, our understanding of this biosynthetic pathway is not complete, hindering its use as a drug target. Recently, we have shown that the pathway involves a new intermediate, (1*R*,2*S*,5*S*,6*S*)-2-succinyl-5-enolpyruvyl-6-hydroxy-3-cyclohexene-1-carboxylate (SEPHCHC,[1] Figure 1) (*6, 7*). The conversion of this intermediate to the next biosynthetic intermediate, (1*R*,6*R*)-2-succinyl-6-hydroxy-2,4-cyclohexadiene-1-carboxylate (SHCHC), requires an additional enzyme whose SHCHC synthase activity has been detected in the crude extract of *Escherichia coli* (*6*). Identification of this SHCHC synthase is a critical step to complete our understanding of this important biosynthetic pathway.

The mechanism of the reaction catalyzed by the SHCHC synthase is proposed as shown in Figure 1B based on the spontaneous decomposition of SEPHCHC to SHCHC (*6*). This enzymatic reaction resembles those catalyzed by Δ^3-Δ^2-enoyl-CoA isomerases (ESIs) (*8, 9*) and Δ^5-3-ketosteroid isomerases (KSIs) (*10–13*). First of all, these reactions are all initiated by abstraction of an α-proton from a carbonyl group in the substrate. Moreover, they all form a dienolate/dienolic intermediate and produce a conjugated product from a nonconjugated substrate (Figure 1). Furthermore, all of the abstracted protons in these enzymatic reactions are flanked by a carbonyl and a carbon double bond and are thus expected to be of comparable acidity. These similarities suggest that the unidentified SHCHC synthase may be homologous to either ESIs or KSIs.

Previous studies have shown that enzymes catalyzing proton-transfer reactions have to overcome an energy barrier, which is related to the acidity of the abstracted proton (*14–17*). This barrier is particularly high for members of the enolase superfamily that abstract low-acidity protons from carboxylate substrates. As a result of this high energetic constraint, the active-site structure of these enzymes is highly conserved (*18, 19*). When this energetic burden is lowered for the reactions catalyzed by the *o*-succinylbenzoate synthase/*N*-acylamino acid racemase (OSBS/NAAAR) family of the enolase super-

[†] This work was financially supported by HKUST and Research Grants Council (RGC) of the Hong Kong SAR government.

* To whom correspondence should be addressed: Department of Chemistry, The Hong Kong University of Science and Technology, Clear Water Bay, Kowloon, Hong Kong SAR, China. Telephone: 852-2358-7352. Fax: 852-2358-1594. E-mail: chguo@ust.hk.

[1] Abbreviations: SEPHCHC, (1*R*,2*S*,5*S*,6*S*)-2-succinyl-5-enolpyruvyl-6-hydroxy-3-cyclohexene-1-carboxylate; SHCHC, (1*R*,6*R*)-2-succinyl-6-hydroxy-2,4-cyclohexadiene-1-carboxylate; ESI, Δ^3-Δ^2-enoyl-CoA isomerase; KSI, Δ^5-3-ketosteroid isomerase; DHNA, 1,4-dihydroxynaphthoate; NHS, *N*-hydroxysuccinimide.

10.1021/bi7023755 CCC: $40.75
Published on Web 02/20/2008

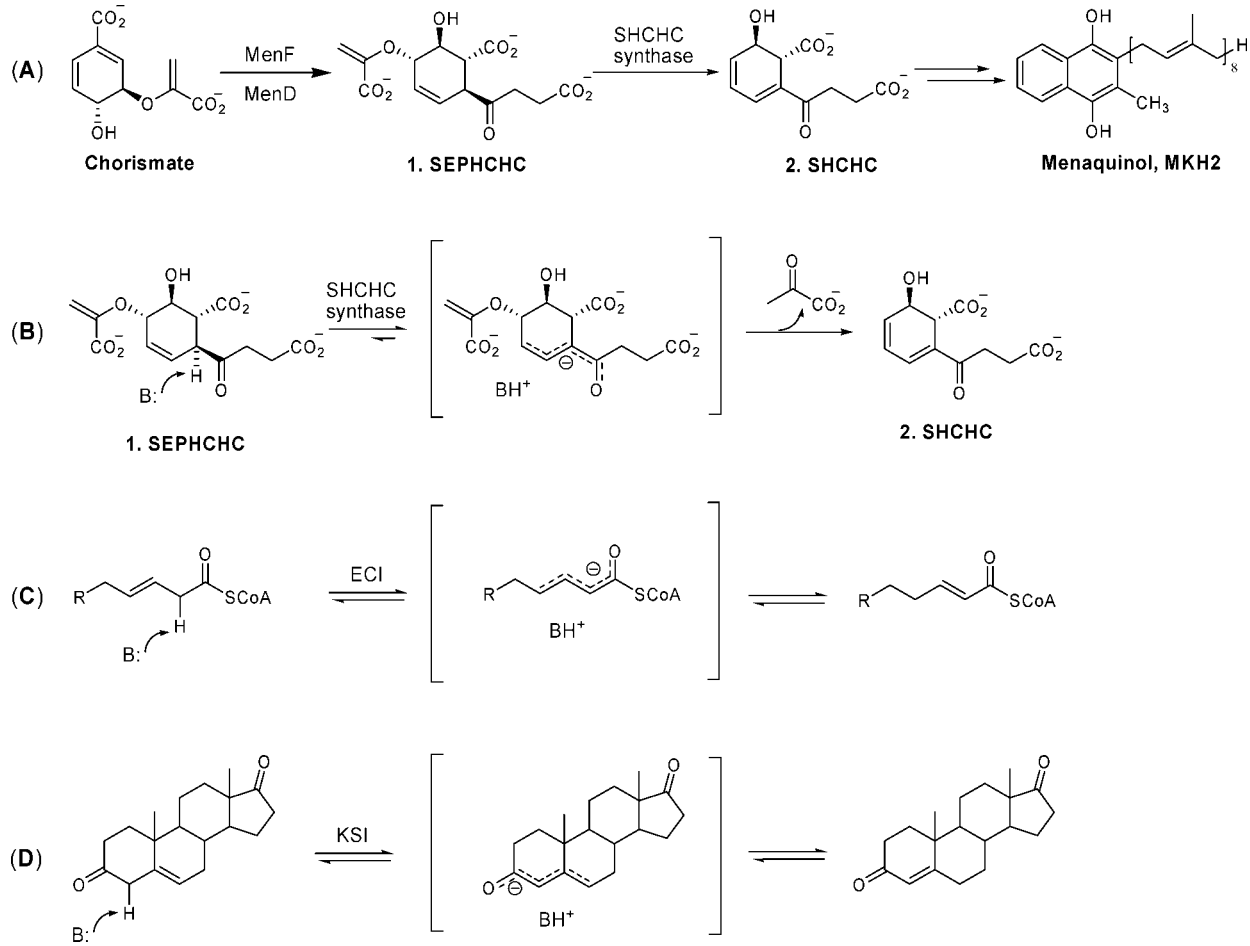

FIGURE 1: SHCHC synthase in the biosynthesis of menquinone and its similarities to other enzymes in catalyzing α-proton abstraction as a partial reaction. (A) Revised menaquinone biosynthetic pathway in *E. coli* with the new intermediate, SEPHCHC. (B) Proposed reaction mechanism for the reaction catalyzed by the SHCHC synthase. (C) Mechanism of the reactions catalyzed by Δ^3-Δ^2-enoyl-CoA isomerases (ESIs). (D) Mechanism of the reactions catalyzed by Δ^5-ketosteroid isomerases (KSIs).

family (*20*), the constraint on the flexibility of the active-site architecture and the sequence divergence is significantly relaxed (*21–26*). For KSIs, ESIs, and the SHCHC synthase, the energetic constraint on the conservation of the structure and sequence is conceivably low because of the high acidity of the abstracted protons in their substrates. Indeed, KSIs are known to have a burden of transition-state stabilization that is similar to members in the OSBS/NAAAR family (*27*). Consistent with this expectation, KSIs and ECIs are two distinct groups of diverse enzymes that share neither sequence homology nor similarities in the active site (*28–31*). In view of this predicted low constraint on sequence and structure diversification, the unknown SHCHC synthase may adopt a structure distinct from that of ESIs or KSIs despite the similarities in the catalytic mechanism.

In search of the SHCHC synthase, we first compared the proteins coded by genes in the proximity of menaquinone biosynthetic genes to ESIs and KSIs. However, no ESI or KSI homologues were found. We finally screened the known menaquinone biosynthetic enzymes and found that MenH, a protein proposed to be a thioesterase catalyzing a later step in the pathway, is the SHCHC synthase. Here, we report its identification and characterization as an enzyme closely related to α/β hydrolases but catalyzing a reaction initiated by proton abstraction.

MATERIALS AND METHODS

General Information. Chemical reagents, including chorismate, α-ketoglutarate, thiamine diphosphate (ThDP), reduced β-nicotinamide adenine dinucleotide (NADH), coenzyme A, adenosine 5′-triphosphate, isopropyl-β-D-thiogalactopyranoside (IPTG), 1,4-dihydroxy-2-naphthoic acid (DHNA), *N*-hydroxysuccinimide (NHS), 1-ethyl-3-(3-dimethylaminopropyl)carbodiimide (EDC) hydrochloride, buffers, and salts were purchased from Sigma. DNA-manipulating biochemicals, including restriction enzymes, T4 DNA ligase, and associated reagents, were obtained from New England Biolabs. Other chemicals and biochemicals in reagent kits were purchased from vendors as specified below. UV–vis absorbance was measured using a Perkin-Elmer Lambda 900 UV/vis/NIR spectrometer. Polymerase chain reaction (PCR) amplifications were performed with a PTC-200 Peltier Thermal Cycler from MJ Research. Protein chromatography was performed on a Bio-Rad BioLogic HR Workstation in a refrigerated chamber. High-performance liquid chromatography (HPLC) analysis and purification were carried out using a Waters 600E system with a Model 2487 dual λ absorbance detector. Nuclear magnetic resonance (NMR) spectrum was taken on a 400 MHz Bruker spectrometer.

Expression and Purification of Enzymes. Expression and

purification of MenC and MenD have been described previously (*6*). Other proteins in the menaquinone biosynthetic pathway were also expressed as a hexahistidine-tagged protein and purified to homogeneity similar to MenC and MenD. The oligodeoxynucleotides used in the gene amplification were CG GGA TCC GTG CAA TCA CTT ACT ACG GCG CTG GAA AA TC (*men*F forward), CA CTC GAG CTA TTC CAT TTG TAA TAA AGT ACG C (*men*F reverse), CCGC GGATCC ATG ATC TTC TCT GAC TGG CCG TGG CGT C (*men*E forward), GCG GAATTC TTA TTG CTG ACG TTG CAC CCA CTC TTT TAG (*men*E reverse), CCGC GGATCC ATG ATT TAT CCT GAT GAA GCA ATG CTT TAC (*men*B forward), and GCG GAATTC TTA CGG ATT CCG TTT GAA TTT GCT G (*men*B reverse). The gene of the YbdB (or P15) protein of the *E. coli* enterobactin biosynthesis (*32*) was similarly cloned in the same vector, and its product was expressed as a hexahistidine-tagged protein at the N terminus, using the primers G CGC GGATCC ATG ATC CTG CAC GCG CAG GCA AAA CAC G and CCG GAATTC TCA GAA ACG CAA GAT CTG CGC CAG ACT TGC. The recombinant proteins were expressed in BL21 (DE3) in Luria broth containing 0.1 mM IPTG at 18 °C for 16 h and purified to greater than 95% in purity by a combination of metal-chelating chromatography and gel filtration. The purified proteins were quantified by a Coomassie Blue protein assay kit (Pierce) and stored in 50 mM Tris-HCl buffer (pH 7.8) containing 10% glycerol and 50 mM NaCl at −20 °C until use.

Gel Filtration. Gel filtration was carried out on a Amersham Biosciences AKTA FPLC system using a Superose 12 10/300 column (GE Healthcare) at a flow rate of 0.5 mL/min. Protein samples were dissolved in 50 mM Tris-HCl buffer (pH 7.5) in the presence of 50 mM NaCl, 1 mM dithiothreitol, and 1 mM ethylenediaminetetraacetic acid (EDTA). The column was calibrated with the low-molecular-mass column calibration kit from GE Healthcare.

Enzymatic Preparation of SEPHCHC and Chemical Synthesis of DHNA−CoA. The preparation of SEPHCHC was carried out as previously described (*6*). A two-step procedure was used to prepare DHNA−CoA from DHNA. The first step was carried out in 5 mL of tetrahydrofuran (THF) containing 204 mg of DHNA (1 mmol), 230 mg of NHS (2 mmol), and 384 mg of EDC (2 mmol). The mixture was stirred at room temperature for 7 h in a nitrogen atmosphere. The organic solvent of the reaction mixture was then evaporated under reduced pressure, and the residue was separated over silica gel and eluted with ethyl acetate/hexane (1:1) to obtain 184 mg of DHNA−NHS (61% yield). A reported procedure (*33*) was then used for thioesterification in the second step. In a stirred solution of the DHNA−NHS ester (32 mg, 0.1 M) in 1.5 mL of THF was added 1.5 mL of coA-SH (20 mg, 0.026 mmol), and the resulting solution was adjusted to pH 8.0 by adding 1 N NaOH and stirred at room temperature for 1 h in a nitrogen atmosphere. After evaporation of the organic solvent under reduced pressure, the residue from the reaction mixture was purified with an Xterra preparative C18 reverse-phase column (10 μm particle size, 19 × 150 mm) on a Waters 600 HPLC system and a linear gradient from (90% A plus 10% B) to (50% A plus 50% B) over 40 min at a flow rate of 7 mL/min. Solution A was a 50 mM aqueous solution of ammonium acetate at pH 5.9, and solution B was 100% methanol. The fractions containing DHNA−CoA were pooled, concentrated under reduced pressure to remove methanol, and then lyophilized to obtain 6.3 mg of product (25% yield). ^{1}H NMR (methanol-d_4, 400 MHz) of DHNA−CoA δ: 8.56 (s, 1H, adenine H), 8.33 (d, J = 8.1 Hz, 1H, adenine H), 8.16 (s, 2H), 7.62 (m, 1H), 7.53 (m, 1H), 6.14 (d, J = 6.0 Hz, 1H, ribose anomeric H), 4.74 (s, 2H), 4.49 (s, 1H, ribose H), 4.28 (s, 2H, ribose CH_2O), 4.09 (s, 2H), 3.59 (m, 1H), 3.56 (m, 1H), 3.49 (m, 2H), 3.47 (m, 2H), 2.45 (t, J = 6.6 Hz, 2H), 1.07 (s, 3H, Me), 0.83 (s, 3H, Me). MS (FAB+): m/z calcd for $C_{32}H_{43}N_7O_{19}P_3S$ $[M + H]^+$, 954.15; found, 954.20.

Enzyme Activity Assays. In the screen for the SHCHC synthase activity, the menaquinone biosynthetic enzymes were assayed in 50 mM sodium phosphate buffer (pH 7.0) containing 5 mM $MgSO_4$ and 50 μM SEPHCHC. The reactions were initiated by adding the enzymes and monitored in real time for change of the absorbance at 293 nm. After 30 min of the reaction at room temperature and subsequent removal of the enzymes by ultrafiltration, the reaction mixtures were analyzed using a Nova-Pak C18 column (4 μm particle size, 3.9 × 150 mm) and isocratic elution with 1% formic acid in water at 1 mL/min. A SHCHC sample from a previous study (*6*) was used as a standard in the HPLC analysis.

HPLC-purified SHCHC from a previous study (*6*) was used to prepare solutions for measurement of absorbance at 290 or 293 nm in reassessment of the SHCHC extinction coefficient (ϵ). These solutions were subsequently added to 100 μM 3,5-dihydroxybenzoic acid (DHB) as an internal control and subject to HPLC analysis under the previously described conditions (*6*). The elution peak area of SHCHC relative to that of the internal control was then used to determine the molar concentration of SHCHC in the original solution to calculate ϵ_{290} or ϵ_{293}, using a calibration curve obtained from similar HPLC analysis of a series of SHCHC solutions with known concentrations and in the presence of 100 μM DHB. To prepare the reference SHCHC solutions, a known amount of chorismate was converted to SHCHC in 600 μL of reaction mixture, which contained 12.5 mM chorismate, 30 μM MenF, 30 μM MenD, 15 μM MenH, 50 mM 2-ketoglutarate, 75 μM thiamine diphosphate, and 7.5 mM $MgSO_4$ in 50 mM sodium phosphate buffer (pH 7.0). After incubation at 37 °C for 2 h, the chorismate−SHCHC conversion was found to be complete by HPLC analysis.

The extinction coefficient of SHCHC at 290 nm was determined to be $(1.28 \pm 0.01) \times 10^4$ M^{-1} cm^{-1}, which is substantially larger than the reported value of 4000 M^{-1} cm^{-1} (*21*). This coefficient was used in the steady-state kinetic study of the SHCHC synthase activity of MenH in 50 mM sodium phosphate buffer (pH 7.0) containing 0.1% BSA. Control assays without enzyme were performed in the same buffer, and the absorbance changes caused by the spontaneous conversion of SEPHCHC to SHCHC were subtracted from the value for the enzymic reactions. All kinetic measurements were carried out in triplicate at 37 ± 0.5 °C.

A reported method (*34*) was modified for the measurement of the MenH thioesterase activity toward palmitoyl-CoA. The newly released free thiol was monitored in real time at 412 nm in the presence of excess Ellman's reagent (dithio-bis-nitrobenzoic acid, DTNB). The assay was carried out in phosphate buffer (pH 7.5) containing 5 mM $MgSO_4$, 100

μM palmitoyl-CoA, and 3 μg/mL MenH or other proteins. The hydrolytic activity of MenH or other proteins toward 50 μM DHNA-CoA was determined by the decrease of the substrate absorbance at 392 nm, following a published method (*3*). The reaction mixtures from the DHNA−CoA hydrolysis were analyzed with a Nova-Pak C18 analytical column (4 μm particle size, 3.9 × 150 mm) and the linear gradient used in the purification of DHNA−CoA at a flow rate of 1 mL/min. Proteins in the reaction product mixtures were removed by ultrafiltration using Amicon YM-10 (Millipore) before HPLC analysis.

Site-Directed Mutagenesis. The QuikChange site-directed mutagenesis kit (Stratagene) was used to replace Ser86, Asp210, or His232 of MenH with alanine. The plasmid obtained above for the expression of MenH was used as the template in the mutagenic reactions. Oligodeoxynucleotides carrying the mutated sequences are C TGG CTG GTG GGG TAC GCA CTT GGT GGA CGG GTG (S86A forward), CAC CCG TCC ACC AAG TGC GTA CCC CAC CAG CCA G (S86A reverse), GT GGT GAA CGT GCT AGC AAA TTC CGC GCC CTG (D210A forward), CAG GGC GCG GAA TTT GCT AGC ACG TTC ACC AC (D210A reverse), C ATT CCT CGC GCC GGC GCT AAC GCG CAT CGG G (H232A forward), and C CCG ATG CGC GTT AGC GCC GGC GCG AGG AAT G (H232A reverse).

RESULTS AND DISCUSSION

Expression and Purification of Menaquinone Biosynthetic Enzymes for the Test of SHCHC Synthase Activity. In principle, the SHCHC synthase can be purified from *E. coli* crude extract to homogeneity according to its activity and identified by subsequent sequencing by Edman degradation or peptide fingerprinting by mass spectroscopy. However, substantial technical difficulty has to be overcome to do this. Before taking this challenge, we first tested whether one of the known enzymes in menaquinone biosynthesis is responsible for the detected SHCHC synthase activity in our previous study (*6*), either as a bifunctional enzyme or as a misdesignated enzyme in the pathway. This test was based on the fact that a biosynthetic enzyme could be involved in discontinuous steps of a pathway, as exemplified by the isochorismatase (EntB) in the biosynthesis of enterobactin (*35, 36*). A positive result from this test could greatly accelerate identification of the missing synthase.

The known menaquinone biosynthetic enzymes MenF, MenD, MenC, MenE, MenB, and MenH were overexpressed in *E. coli* as hexahistidine-tagged proteins and purified to homogeneity by a combination of nickel(II)-affinity chromatography and size-exclusion chromatography (Figure 2A). The integral membrane protein MenA (*37, 38*) was not expressed for the test because the detected SHCHC synthase activity was associated with the nonmembranous supernatant of the crude extract after ultracentrifugation (data not shown). UbiE was not tested because it is a monofunctional enzyme also involved in ubiquinone biosynthesis (*39*).

The purified enzymes were tested for SHCHC synthase activity by a reported continuous assay, relying on the unique absorption of the SHCHC product at 293 nm (*6, 21*). As shown in Figure 2B, MenH exhibited a high level of activity in catalyzing the formation of SHCHC from SEPHCHC. In contrast, all other proteins gave a negligible SHCHC

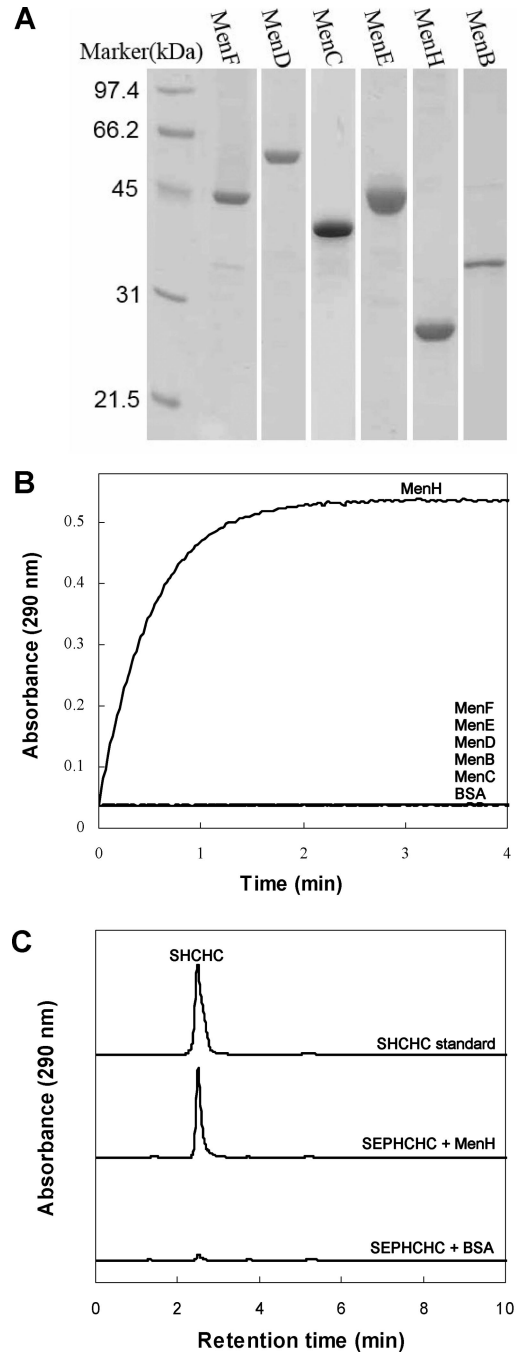

FIGURE 2: Screening the menaquinone biosynthetic enzymes for the SHCHC synthase. (A) Denaturing SDS−PAGE of the purified menaquinone biosynthetic enzymes. (B) Real-time monitoring of SEPHCHC to SHCHC decomposition at 290 nm in the presence of various menaquinone biosynthetic enzymes. (C) HPLC analysis of the reaction mixture of the MenH-catalyzed reaction. Reaction conditions: 50 μM SEPHCHC, 5 mM $MgSO_4$, and 1.5 μg/mL MenH or 10 μg/mL of other enzymes in 50 mM phosphate buffer (pH 7.0) at room temperature.

formation rate that was indistinguishable from the spontaneous SEPHCHC decomposition under the given conditions. The lack of SHCHC synthase activity for MenC and MenD has been demonstrated previously (*6*) and is consistent with the results presented here. The formation of SHCHC in the MenH-catalyzed reaction was further confirmed by HPLC analysis using an authentic sample from a previous study (*6*) (Figure 2C). These results show that the SHCHC synthase

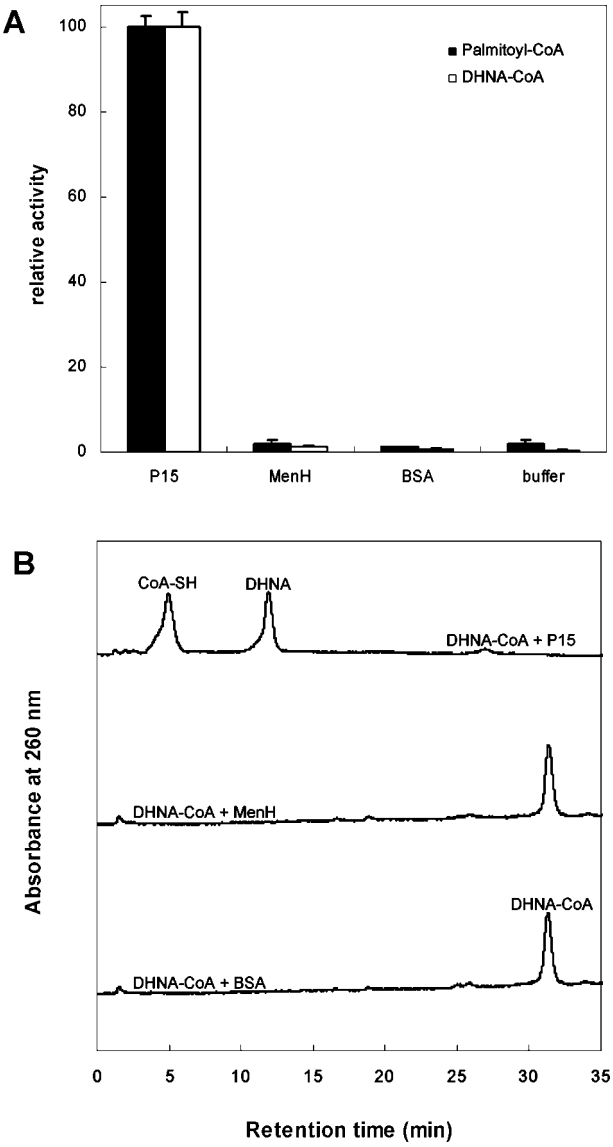

FIGURE 3: MenH lacks thioesterase activity. (A) Normalized thioesterase activity of MenH and controls toward palmitoyl-CoA (open bar) and DHNA−CoA (shaded bar). (B) HPLC analysis of the DHNA−CoA hydrolysis reaction mixtures. The reactions were carried out in 50 mM phosphate buffer (pH 7.0) containing 5 mM $MgSO_4$ and 3.0 μg/mL MenH of other control proteins. Esterase activity toward palmitoyl-CoA was assayed by coupling to DTNB oxidation of the released free thiol, and the DHNA−CoA hydrolytic activity was determined by real-time monitoring of the decrease of absorbance at 392 nm.

is indeed associated with a known enzyme in the menaquinone biosynthetic pathway.

MenH as a Dedicated SHCHC Synthase. MenH was previously proposed to be responsible for the hydrolysis of DHNA−CoA (*2, 21*), a necessary step in menaquinone biosynthesis. The finding of the palmitoyl-CoA hydrolytic activity for MenH (*40*) supports this proposed function. To determine whether MenH is a bifunctional enzyme catalyzing discontinuous steps in menaquinone biosynthesis, its thioesterase activity was reassessed. Its hydrolytic activity toward palmitoyl-CoA was determined with Ellman's reagent to be about the same as that of bovine serum albumin (BSA) or the blank buffer control (Figure 3A). Under identical conditions, a genuine thioesterase, YbdB (also called P15 or EntH) from *E. coli* (*32*), exhibits a thioesterase activity at least 100-fold higher than MenH or the negative controls. This simple test did not support the reported thioesterase activity for MenH.

To directly test the hydrolytic activity of MenH toward its presumed substrate, DHNA−CoA was chemically synthesized, purified by preparative reverse-phase HPLC, and structurally characterized by mass spectrometry and ^{1}H NMR spectrometry. Continuous monitoring of the unique absorbance of DHNA−CoA at 392 nm found that MenH has a lower hydrolytic activity than BSA or the blank buffer toward this substrate, indicating that it completely lacks the proposed thioesterase activity. Because DHNA−CoA tends to be oxidized by air in neutral buffer to form products not detectable by HPLC (data not shown), the incubation product mixtures from the activity assay were subject to HPLC analysis to ensure that DHNA−CoA was not degraded in the assay. As shown in Figure 3C, the substrate DHNA−CoA was intact in the activity assay carried out at pH 7.0, confirming the finding that MenH is unable to hydrolyze DHNA−CoA. Together with the newly found SHCHC synthase activity, these results show that MenH is a monofunctional enzyme committed to SHCHC synthesis in menaquinone biosynthesis.

Quaternary Structure of MenH and Cofactor Requirement. The homogeneous MenH was a single symmetric peak in analytical gel filtration with a Superose 12 10/300 column. After calibration of the column with molecular-weight-marker proteins, the MenH native molecular weight was determined to be 25.4 kDa. In comparison to the calculated monomeric size of 29.7 kDa, MenH is obviously a monomeric protein. The ultraviolet–visible light absorption spectrum of the protein is almost identical to that of BSA, suggesting that the protein is free of a chromogenic cofactor. In addition, the SHCHC synthase activity of MenH was not affected by the addition of a divalent ion (1 mM of Mg^{2+}, Ba^{2+}, Mn^{2+}, Ca^{2+}, Co^{2+}, or Ni^{2+}) or 1 mM EDTA to the assay solution. From these results, MenH is a monomeric enzyme without a cofactor.

Steady-State Kinetics. We used the continuous activity assay based on the increase of SHCHC absorption at 293 nm but found that the extinction coefficient of the product might be underestimated in previous studies (*21*). The coefficient constant was reassessed to be $(1.28 \pm 0.01) \times 10^4$ M^{-1} cm^{-1} using a combination of enzymatic conversion, HPLC analysis, and UV spectroscopy. Using this new constant, the MenH-catalyzed reaction was found to follow standard Michaelis–Menten kinetics (Figure 4). At pH 7.0 and 37 °C in phosphate buffer, MenH is highly active as an SHCHC synthase with a high catalytic efficiency (k_{cat}/K_M = $(2.0 \pm 0.1) \times 10^7$ M^{-1} s^{-1}, $k_{cat} = 167 \pm 1$ s^{-1}, and K_M = 8.3 ± 0.8 μM).

Energetics of MenH Catalysis. According to the proposal that enzyme catalysis stems from the affinity of the enzyme for the transition state (*41*), stabilization of the transition state by MenH can be determined by comparing the rates of the catalyzed and noncatalyzed reactions. The rate constant (k_{non}) of the noncatalyzed decomposition of SEPHCHC to SHCHC is $2.1 \pm 0.1 \times 10^{-5}$ s^{-1} at pH 7.0 and 37 °C in phosphate buffer (*6*). The catalytic proficiency [$(k_{cat}/K_M)/k_{non}$] of MenH is calculated to be 9.8×10^{11} M^{-1}, which corresponds to the stabilization of the enzyme-bound transition state by 17 kcal/mol. To better understand the noncatalyzed reaction,

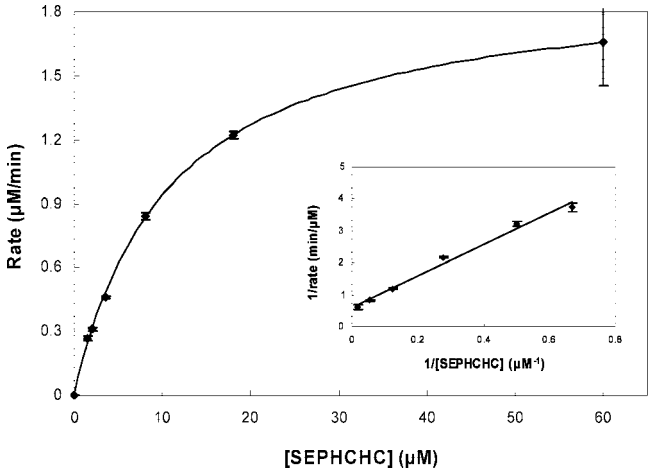

FIGURE 4: Michaelis–Menten kinetics of the MenH-catalyzed reaction. The reactions were carried out in 50 mM phosphate buffer (pH 7.0) at 37 °C. (Inset) Lineweaver–Burk plot from which K_M and k_{cat} were determined.

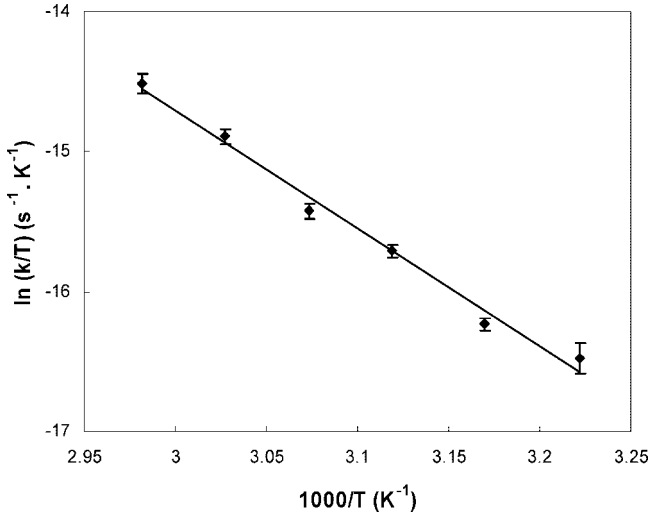

FIGURE 5: Temperature dependence of the spontaneous decomposition of SEPHCHC to SHCHC in phosphate buffer at pH 7.0.

temperature dependence of its first-order rate constant was determined at pH 7.0. The enthalpy change, the entropy change, and the activation energy in transition-state formation at 37 °C were respectively determined to be 18.1 ± 0.6 kcal mol^{-1}, −22.0 ± 1.9 cal mol^{-1} K^{-1}, and 24.9 ± 0.3 kcal mol^{-1} from the plot of ln(k/T) versus ($1/T$) as shown in Figure 5 (*42*). In combination with the free-energy changes calculated for the enzyme–substrate complex formation, the free-energy profile of the MenH-catalyzed reaction is given in Figure 6.

The transition-state stabilization provided by various enzymes catalyzing proton abstraction from carbon acids is listed in Table 1. In comparison to fumarase and mandelate racemase that abstract protons with a pK_a greater than 29, MenH provides less transition-state stabilization by 9–13 kcal/mol. The stabilization of MenH of the transition state is also 4 kcal/mol lower than OSBS synthase or KSI that abstract protons with a pK_a similar to that of the transferred proton in the substrate of MenH. This comparison shows that MenH has a smaller "burden" than other proton-abstracting enzymes to stabilize the transition state to achieve a high catalytic efficiency ($k_{cat}/K_M \approx 10^6-10^8$ M^{-1} s^{-1}). To test whether this low energetic burden may be due to the

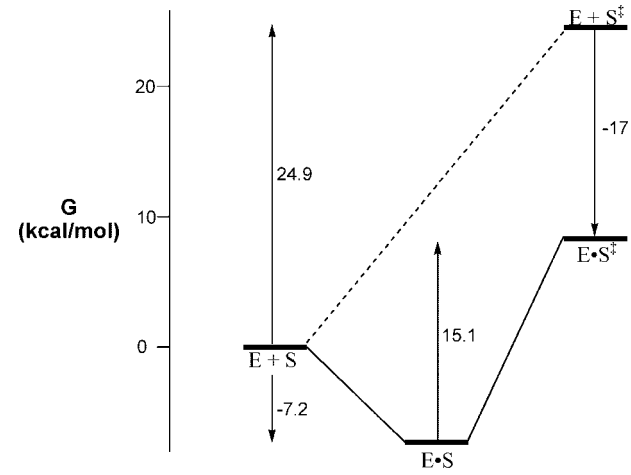

FIGURE 6: Free-energy profile (pH 7.0 and 37 °C) for the SHCHC synthesis in the absence of an enzyme (- - -) and in the presence of MenH (—). The energy of the ES complex is calculated from $\Delta G = RT \ln(K_M)$, assuming that K_M is the dissociation constant of the complex.

high acidity of the abstracted proton in SEPHCHC, the spontaneous decomposition rate of SEPHCHC was titrated with the pH value of the reaction buffer as demonstrated previously (*6*). Unfortunately, the rate continuously increases with an increasing pH value up to pH 14.0 (data not shown) and does not allow for a confident estimation of the pK_a of the acidic proton. Nevertheless, the small transition-state stabilization for MenH suggests a low constraint on the diversification of its sequence and structure in evolution. Indeed, MenHs are the most diverse proteins among menaquinone biosynthetic enzymes from different species (*26*).

Comparison of MenH with Homologous Enzymes. Interestingly, the crystallographic structure of MenH in the menaquinone biosynthetic cluster of *Vibrio cholarae*, which was identified on the basis of a combination of genomic context and homology of the highly conserved DHNA−CoA synthase (*26*), has been determined as an unknown protein [Protein Data Bank (PDB) 1R3D]. The pairwise amino acid identity between this protein and *E. coli* MenH is 40%. The closest structural homologue of this cholarae protein is MhpC, which is a well-characterized C−C bond α/β hydrolase from *E. coli* (*50, 51*). As shown in Figure 7A, the overall topology of MenH and MhpC is very similar: the core region is a central β sheet of eight strands flanked by several small and short α helices on both sides, which is capped by a four-helix domain that most likely controls the access of the substrate. A major difference is the presence of an additional β strand at the N terminus of the core β sheet in the MenH structure. Another difference lies in the exact orientation and length of the α helices flanking the core β sheet or the α helices in the capping domain.

More significantly, the Ser-His-Asp catalytic triad of MhpC (*50, 51*) is conserved in a sequence alignment of the protein with MenHs from both *E. coli* and *V. cholarae*. The corresponding residues of the MhpC triad in *E. coli* MenH, Ser86, Asp210, and His232, were found to be conserved in all 40 identified MenH proteins (*26*) in a multisequence alignment (data not shown). Examination of these three residues in the *V. cholarae* MenH structure or the modeled structure of *E. coli* MenH (Figure 7B) found that they indeed

Table 1: Transition-State Stabilization (ΔG_{TX}) of MenH and Other Enzymes Catalyzing Proton Abstraction from Carbon Acids

enzyme	substrate	pK_a	k_{cat}/K_M (M^{-1} s^{-1})[a]	k_{non} (s^{-1})[b]	ΔG_{TX} (kcal mol^{-1})
mandelate racemase[c]	(*R*)-mandelate	~29[d]	1.3×10^6	3.0×10^{-13}	−26
fumarase[c]	(*S*)-malate	22–30[d]	7.1×10^7	7.6×10^{-14}	−30
triose-phosphate isomerase[c]	glyceraldehydes-3-phosphate	~17[d]	2.4×10^8	4.3×10^{-6}	−19
o-succinylbenzoate synthase[e]	SHCHC		1.8×10^6	1.6×10^{-10}	−22
Δ^5-3-ketosteroid isomerase[c]	5-androstene-3,17-dione	12.7[f]	3.0×10^8	1.7×10^{-7}	−21
SHCHC synthase (MenH)	SEPHCHC		2.0×10^7	2.1×10^{-5}	−17

[a] Enzymic kinetic data were obtained for mandelate racemase from ref *44*, for fumarase from ref *45*, for triose-phosphate isomerase from ref *46*, and for ketosteroid isomerase from ref *47*. [b] Nonenzymatic rate constants were obtained for (*R*)-mandelate from ref *27*, for (*S*)-malate from ref *45*, for glyceraldehydes 3-phosphate from ref *48*, and for ketosteroid isomerase from ref *49*. [c] Data taken from ref *27*; see the following footnotes for original references. [d] Data from ref *14*. [e] Data from ref *20*. [f] Data from ref *43*.

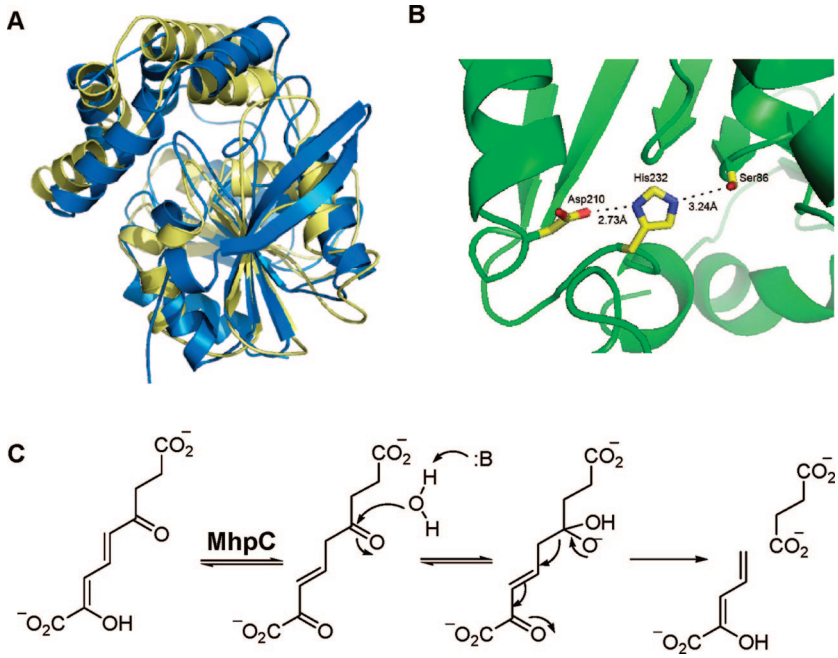

FIGURE 7: (A) Superposition of the X-ray crystallographic structures of the C−C bond hydrolase MhpC (yellow) and the MenH protein from *V. cholerae* (blue). (B) Ser-His-Asp triad in the *E. coli* MenH structure modeled from the crystallographic structure of the *V. cholerae* protein. (C) Reactions catalyzed by the C−C bond hydrolase MhpC. PDB numbers 1U2E (MhpC) and 1R3D (*V. cholerae* MenH). SWISS-MODEL was used for the structural superposition and modeling.

form a triad closely resembling that of MhpC through hydrogen bonding. These structural and sequential similarities between MenH and MhpC are likely the basis of the previously proposed MenH role as a DHNA−CoA thioesterase (*2, 21*) and the functional annotation of the MenH proteins as "predicted hydrolases or acyltransferases" (α/β hydrolases superfamily) in GenBank. However, although these similarities show that it is indeed closely related to α/β hydrolases, MenH catalyzes a reaction that is mechanistically different from the reactions catalyzed by all members of the α/β hydrolase superfamily (*52*).

Dependence of MenH Catalysis on the Ser-His-Asp Triad. An interesting question about the presence of a well-conserved Ser-His-Asp triad in MenH is whether it contributes to the catalysis of proton transfer in SHCHC synthesis. Thus far, two catalytic patterns have been known for Ser-His-Asp catalytic triads. First of all, the triad of serine proteases is invariably involved in the generation of a seryl nucleophile for subsequent addition to the scissile amide bond of the substrates. This catalytic role, however, is apparently not needed in the enzymatic SHCHC synthesis by MenH. Second, the MhpC triad catalyzes C−C bond cleavage (Figure 7C) in a very different way; its serine residue has a non-nucleophilic role, while the histidine residue serves as a general base to catalyze keto–enol tautomerization in the first half-reaction and to abstract a proton from water in the subsequent C−C bond cleavage (*50*). On the basis of the structural and sequential similarities with MhpC, MenH may use the histidine residue of its triad as a catalytic base to initiate the 2,5-elimination of pyruvate, similar to the abstraction of the MhpC triad of an α-proton from a carbon acid in the reverse enolization of the first half-reaction.

To examine the significance of this *E. coli* MenH triad to the SHCHC synthase activity, the three amino acid residues were individually replaced by alanine using site-directed mutagenesis. All three site-directed mutants present a far-UV circular dichroism spectrum that overlaps that of the wild-type protein (data not shown), indicating that the MenH conformation is minimally affected by the point mutations. Kinetic characterization found a low level of residual activity for the serine-to-alanine mutant (1400-fold decrease in k_{cat}/K_M, Table 2). However, the SHCHC synthase activity is essentially eliminated for the other two mutants. These activity data are consistent with a nonessential role for the serine residue, similar to the non-nucleophilic role for the serine residue in the MhpC triad, and a critical role for the histidine as a catalytic base in MenH catalysis. Indeed, this mutational analysis clearly demonstrates that the Ser-His-

Table 2: Steady-State Kinetic Parameters for Wild-Type MenH and Its Mutants at 25 °C

variant	K_M (μM)	k_{cat} (s^{-1})	k_{cat}/K_M (M^{-1} s^{-1})	relative k_{cat}/K_M
wild type	10.1 ± 0.8	147 ± 9	$1.4 \pm 0.5 \times 10^7$	1
S86A	28 ± 3	0.29 ± 0.01	$1.0 \pm 0.1 \times 10^4$	7.1×10^{-4}
D210A	118 ± 22	0.18 ± 0.02	$1.5 \pm 0.2 \times 10^3$	1.1×10^{-4}
H232A	8.6 ± 0.3	$5.8 \pm 0.7 \times 10^{-4}$	67 ± 10	4.8×10^{-6}

Asp triad is essential to the activity of MenH and suggests that it is at least partly similar to the MhpC triad in catalytic functions. Nevertheless, the MhpC triad is still committed to generating a nucleophile to attack a carbonyl group in the second half-reaction (*50*), whereas the MenH triad is surely lacking of this function because a nucleophile is not involved in the SHCHC synthesis by MenH. This distinction predicts that the MenH triad plays catalytic roles different from the corresponding triads in either serine proteases or α/β hydrolases.

CONCLUSIONS

We have successfully identified MenH of the menaquinone biosynthetic enzyme cluster as the SHCHC synthase that efficiently converts the SEPHCHC intermediate to SHCHC. This protein is not the DHNA−CoA thioesterase as previously proposed (*2, 21*) because of its lack of thioesterase activity toward either acyl-CoA or the proposed substrate. A logical extension of this result is that a new DHNA−CoA thioesterase is yet to be found to fully account for the biosynthesis of menaquinone.

MenH was found to have a smaller energetic burden to stabilize the transition state than other enzymes catalyzing abstraction of α-protons from carbon acids. This low energetic requirement may underlie the high diversity of the MenH proteins from different species. Despite being devoid of thioesterase activity, MenH closely resembles the α/β hydrolases in overall three-dimensional structure and contains a Ser-His-Asp triad typical of serine proteases. Interestingly, this triad is essential for the SHCHC synthase activity of MenH, suggesting that it plays a crucial role in the proton-abstraction reaction, which is distinct from its well-known function in the catalysis of serine proteases. Elucidation of the mechanistic role of this MenH motif will provide a unique opportunity to fully appreciate the catalytic potential of the classic catalytic triad.

REFERENCES

1. Meganathan, R. (1996) Biosynthesis of the isoprenoid quinones menaquinone (vitamin K_2) and ubiquinone (coenzyme Q), in *Escherichia coli and Salmonella: Cellular and Molecular Biology*, 2nd ed. (Neidhardt, F. C., Curtis, R., III, Ingraham, J. L., Lin, E. C. C., Low, K. B., Magasanik, B., Reznikoff, W. S., Riley, M., Schaechter, M., and Umbarger, H. E., Eds.) Vol. 1, pp 642–656, American Society for Microbiology, Washington, D.C.
2. Meganathan, R. (2001) Biosynthesis of menaquinone (vitamin K_2) and ubiquinone (coenzyme Q): A perspective on enzymatic mechanisms. *Vitam. Horm. 61*, 173–218.
3. Truglio, J. J., Theis, K., Feng, Y., Gajda, R., Machutta, C., Tonge, P. J., and Kisker, C. (2003) Crystal structure of *Mycobacterium tuberculosis* MenB, a key enzyme in vitamin K_2 biosynthesis. *J. Biol. Chem. 278*, 42352–42360.
4. Johnston, J. M., Arcus, V. L., and Baker, E. N. (2005) Structure of naphthoate synthase (MenB) from *Mycobacterium tuberculosis* in both native and product-bound forms. *Acta Crystallogr., Sect. D: Biol. Crystallogr. 61*, 1199–1206.
5. Kurosu, M., Narayanasamy, P., Biswas, K., Dhiman, R., and Crick, D. C. (2007) Discovery of 1,4-dihydroxy-2-naphthoate prenyltransferase inhibitors: New drug leads for multidrug-resistant Gram-positive pathogens. *J. Med. Chem. 50*, 3973–3975.
6. Jiang, M., Cao, Y., Guo, Z.-F., Chen, M., Chen, X., and Guo, Z. (2007) Menaquinone biosynthesis in *Escherichia coli*: Identification of 2-succinyl-5-enolpyruvyl-6-hydroxy-3-cyclohexene-1-carboxylate (SEPHCHC) as a novel intermediate and re-evaluation of MenD activity. *Biochemistry 46*, 10979–10989.
7. Jiang, M., Chen, M., Cao, Y., Yang, Y., Sze, K. H., Chen, X., and Guo, Z. (2007) Determination of the stereochemistry of 2-succinyl-5-enolpyruvyl-6-hydroxy-3-cyclohexene-1-carboxylic acid, a key intermediate in menaquinone biosynthesis. *Org. Lett. 9*, 4765–4767.
8. Müller-Newen, G., and Stoffel, W. (1993) Site-directed mutagenesis of putative active-site amino acid residues of 3,2-trans-enoyl-CoA isomerase, conserved within the low-homology isomerase/hydratase enzyme family. *Biochemistry 32*, 11405–11412.
9. Müller-Newebm, G., Janssen, U., and Stoffel, W. (1995) Enoyl-CoA hydratase and isomerase form a superfamily with a common active-site glutamate residue. *Eur. J. Biochem. 228*, 68–73.
10. Kuliopulos, A., Mildvan, A. S., Shortle, D., and Talalays, P. (1989) Kinetic and ultraviolet spectroscopic studies of active-site mutants of Δ^5-3-ketosteroid isomerase. *Biochemistry 28*, 149–159.
11. Xue, L., Talalay, P., and Mildvan, A. S. (1990) Studies of the mechanism of the Δ^5-3-ketosteroid isomerase reaction by substrate, solvent, and combined kinetic deuterium isotope effects on wild-type and mutant enzymes. *Biochemistry 29*, 7491–7500.
12. Kuliopulos, A., Talalay, P., and Mildvan, A. S. (1990) Combined effects of two mutations of catalytic residues on the ketosteroid isomerase reaction. *Biochemistry 29*, 10271–10280.
13. Hawkinson, D. C., and Pollack, R. M., Jr. (1994) Evaluation of the internal equilibrium constant for 3-oxo-Δ^5-steroid isomerase using the D38E and D38N mutants: The energetic basis for catalysis. *Biochemistry 33*, 12172–12183.
14. Gerlt, J. A., Kozarich, J. W., Kenyon, G. L., and Gassman, P. G. (1991) Electrophilic catalysis can explain the unexpected acidity of carbon acids in enzyme-catalyzed reactions. *J. Am. Chem. Soc. 113*, 9667–9669.
15. Gerlt, J. A., and Gassman, P. G. (1992) Understanding enzyme-catalyzed proton abstraction from carbon acids: Details of stepwise mechanisms for β-elimination reactions. *J. Am. Chem. Soc. 114*, 5928–5934.
16. Gerlt, J. A., and Gassman, P. G. (1993) An explanation for rapid enzyme-catalyzed proton abstraction from carbon acids: Importance of late transition states in concerted mechanisms. *J. Am. Chem. Soc. 115*, 11552–11568.
17. Gerlt, J. A., and Gassman, P. G. (1993) Understanding the rates of certain enzyme-catalyzed reactions: Proton abstraction from carbon acids, acyl-transfer reactions, and displacement reactions of phosphodiesters. *Biochemistry 32*, 11943–11952.
18. Gerlt, J. A., and Babbitt, P. C. (2001) Divergent evolution of enzymatic functions: Mechanistically diverse superfamilies and functionally distinct superfamilies. *Annu. Rev. Biochem. 70*, 209–246.
19. Gerlt, J. A., Babbitt, P. C., and Rayment, I. (2005) Divergent evolution in the enolase superfamily: The interplay of mechanism and specificity. *Arch. Biochem. Biophys. 433*, 59–70.
20. Taylor, E. A., Palmer, D. R. J., and Gerlt, J. A. (2001) The lesser "burden born" by *o*-succinylbenzoate synthase: An "easy" reaction involving a carboxylate carbon acid. *J. Am. Chem. Soc. 123*, 5824–5825.
21. Palmer, D. R. J., Garrett, J. B., Sharma, V., Meganathan, R., Babbitt, P. C., and Gerlt, J. A. (1999) Unexpected divergence of enzyme function and sequence: "*N*-Acylamino acid racemase" is *o*-succinylbenzoate synthase. *Biochemistry 38*, 4252–4258.
22. Thompson, T. B., Garrett, J. B., Taylor, E. A., Meganathan, R., Gerlt, J. A., and Rayment, I. (2000) Evolution of enzymatic activity in the enolase superfamily: Structure of *o*-succinylbenzoate synthase from *Escherichia coli* in complex with Mg^{2+} and *o*-succinylbenzoate. *Biochemistry 39*, 10662–10676.
23. Klenchin, V. A., Ringia, E. A. T., Gerlt, J. A., and Rayment, I. (2003) Evolution of enzymatic activity in the enolase superfamily: Structural and mutagenic studies of the mechanism of the reaction catalyzed by *o*-succinylbenzoate synthase from *Escherichia coli*. *Biochemistry 42*, 14427–14433.
24. Ringia, E. A. T., Garrett, J. B., Thoden, J. B., Holden, H. M., Rayment, I., and Gerlt, J. A. (2004) Evolution of enzymatic activity

in the enolase superfamily: Functional studies of the promiscuous *o*-succinylbenzoate synthase from *Amycolatopsis*. *Biochemistry 43*, 224–229.
25. Thoden, J. B., Ringia, E. A. T., Garrett, J. B., Gerlt, J. A., Holden, H. M., and Rayment, I. (2004) Evolution of enzymatic activity in the enolase superfamily: Structural studies of the promiscuous *o*-succinylbenzoate Synthase from *Amycolatopsis*. *Biochemistry 43*, 5716–5727.
26. Glasner, M. E., Fayazmanesh, N., Chiang, R. A., Sakai, A., Jacobson, M. P., Gerlt, J. A., and Babbitt, P. C. (2006) Evolution of structure and function in the *o*-succinylbenzoate synthase/*N*-acylamino acid racemase family of the enolase superfamily. *J. Mol. Biol. 360*, 228–250.
27. Bearne, S. L., and Wolfenden, R. (1997) Mandelate racemase in pieces: Effective concentration of enzyme functional groups in the transition state. *Biochemistry 36*, 1646–1656.
28. Mursula, A. M., van Aalten, D. M. F., Hiltunen, J. K., and Wierenga, R. K. (2001) The crystal structure of Δ^3-Δ^2-enoyl-CoA isomerase. *J. Mol. Biol. 309*, 845–853.
29. Hubbard, P. A., Yu, W., Schulz, H., and Kim, J.-J. P. (2005) Domain swapping in the low-similarity isomerase/hydratase superfamily: The crystal structure of rat mitochondrial Δ^3,Δ^2-enoyl-CoA isomerase. *Protein Sci. 14*, 1545–1555.
30. Kuliopulos, A., Westbrook, E. M., Talalay, P., and Mildvan, A. S. (1987) Positioning of a spin-labeled substrate analogue into the structure of Δ^5-3-ketosteroid isomerase by combined kinetic, magnetic resonance, and X-ray diffraction methods. *Biochemistry 26*, 3927–3937.
31. Westbrook, E. M., Piro, O. E., and Sigler, P. B. (1984) The 6 Å crystal structure of Δ^5-3-ketosteroid isomerase. *J. Biol. Chem. 259*, 9096–9103.
32. Leduc, D., Battesti, A., and Bouveret, E. (2007) The hotdog thioesterase EntH (YbdB) plays a role in vivo in optimal enterobactin biosynthesis by interacting with the ArCP domain of EntB. *J. Bacteriol. 189*, 7112–7126.
33. Lai, M.-t., Li, D., Oh, E., and Liu, H.-w. (1993) Inactivation of medium-chain acyl-CoA dehydrogenase by a metabolite of hypoglycin: Characterization of the major turnover product and evidence suggesting an alternative flavin modification pathway. *J. Am. Chem. Soc. 115*, 1619–1628.
34. Zhou, Y., Guo, X. C., Yi, T., Yoshimoto, T., and Pei, D. (2000) Two continuous spectrophotometric assays for methionine aminopeptidase. *Anal. Biochem. 280*, 159–165.
35. Rusnak, F., Liu, J., Quinn, N., Berchtold, G. A., and Walsh, C. T. (1990) Subcloning of the enterobactin biosynthetic gene entB: Expression, purification, characterization, and substrate specificity of isochorismatase synthase. *Biochemistry 29*, 1425–1435.
36. Gehring, A. M., Bradley, K. A., and Walsh, C. T. (1997) Enterobactin biosynthesis in *Escherichia coli*: Isochorismate lyase (EntB) is a bifunctional enzyme that is phosphopantetheinylated by EntD and then acylated by EntE using ATP and 2,3-dihydroxybenzoate. *Biochemistry 36*, 8495–8503.
37. Shineberg, B., and Young, I. G. (1976) Biosynthesis of bacterial menaquinones: The membrane associated 1,4-dihydroxy-2-naphthoate octaprenyltransferase of *Escherichia coli*. *Biochemistry 15*, 2754–2758.
38. Suvarna, K., Stevenson, D., Meganathan, R., and Hudspeth, M. E. S. (1998) Menaquinone (vitamin K_2) biosynthesis: Localization and characterization of the menA gene from *Escherichia coli*. *J. Bacteriol. 180*, 2782–2787.
39. Lee, P. T., Hsu, A. Y., Ha, H. T., and Clarke, C. F. (1997) A *C*-methyltransferase involved in both ubiquinone and menaquinone biosynthesis: Isolation and identification of the *Escherichia coli* ubiE gene. *J. Bacteriol. 179*, 1748–1754.
40. Kuznetsova, E., Proudfoot, M., Sanders, S. A., Reinking, J., Savchenko, A., Arrowsmith, C. H., Edwards, A. M., and Yakunin, A. F. (2005) Enzyme genomics: Application of general enzymatic screens to discover new enzymes. *FEMS Microbiol. Rev. 29*, 263–279.
41. Bruice, T. C., and Benkovic, S. J. (2000) Chemical basis for enzyme catalysis. *Biochemistry 39*, 6267–6274.
42. Cleland, W. W., and Northrop, D. B. (1999) Energetics of substrate binding, catalysis, and product release. *Methods Enzymol. 308*, 3–27.
43. Zeng, B., and Pollack, R. M. (1991) Microscopic rate constants for the acetate ion catalyzed isomerization of 5-androstene-3,17-dione to 4-androstene-3,17-dione: A model for steroid isomerase. *J. Am. Chem. Soc. 113*, 3838–3842.
44. Mitra, B., Kallarakal, A. T., Kozarich, J. W., Gerlt, J. A., Clifton, J. G., Pesko, G. A., and Kenyon, G. L. (1995) Mechanism of the reaction catalyzed by mandelate racemase: Importance of electrophilic catalysis by glutamic acid 317. *Biochemistry 34*, 2777–2787.
45. Bearne, S. L., and Wolfenden, R. (1995) Enzymatic hydration of an olefin: The burden borne by fumarase. *J. Am. Chem. Soc. 117*, 9588–9589.
46. Putman, S. J., Coulson, A. F., Farley, I. R., Riddleston, B., and Knowles, J. R. (1972) Specificity and kinetics of triose phosphate isomerase from chicken muscle. *Biochem. J. 129*, 301–310.
47. Pollack, R. M., Zeng, B., Mack, J. P. G., and Eldin, S. (1989) Determination of the microscopic rate constants for the base-catalyzed conjugation of 5-androstene-3,17-dione. *J. Am. Chem. Soc. 111*, 6419–6423.
48. Hall, A, and Knowles, J. R. (1975) The uncatalyzed rates of enolization of dihydroxyacetone phosphate and of glyceraldehyde 3-phosphate in neutral aqueous solution. The quantitative assessment of the effectiveness of an enzyme catalyst. *Biochemistry 14*, 4348–4353.
49. Hawkinson, D. C., Eames, T. C., and Pollack, R. M. (1991) Energetics of 3-oxo-Δ^5-steroid isomerase: Source of the catalytic power of the enzyme. *Biochemistry 30*, 10849–10858.
50. Li, C., Montgomery, M. G., Mohammed, F., Li, J.-J., Wood, S. P., and Bugg, T. D. H. (2005) Catalytic mechanism of C−C hydrolase MhpC from *Escherichia coli*: Kinetic analysis of His263 and Ser110 site-directed mutants. *J. Mol. Biol. 346*, 241–251.
51. Dunn, G., Montgomery, M. G., Mohammed, F., Coker, A., Cooper, J. B., Robertson, T., Garcia, J.-L., Bugg, T. D. H., and Wood, S. P. (2005) The structure of the C−C bond hydrolase MhpC provides insights into its catalytic mechanism. *J. Mol. Biol. 346*, 253–265.
52. Holmquist, M. (2000) α/β-Hydrolase fold enzymes: Structure, functions and mechanisms. *Curr. Protein Pept. Sci. 1*, 209–235.

BI7023755